Proceedings of the International Symposium on Engineering Lessons Learned from
the 2011 Great East Japan Earthquake, March 1-4, 2012, Tokyo, Japan

SEISMOLOGICAL AND GEODETIC ASPECTS OF THE 2011 TOHOKU EARTHQUAKE AND GREAT EAST JAPAN EARTHQUAKE DISASTER

Kazuki KOKETSU[1]

[1] Professor, Earthquake Research Institute, University of Tokyo,
Tokyo, Japan, koketsu@eri.u-tokyo.ac.jp

ABSTRACT: One general feature and three specific features were pointed out for the 2011 Tohoku earthquake and Great East Japan Earthquake Disaster. The three specific features are: (1) "Observed by dense networks of geophysical instruments," (2) "Severe tsunami damage but moderate ground motion damage", and (3) "They had not been forseen at all." These have been explained in detail as the seismological and geodetic aspects of the 2011 Tohoku earthquake and Great East Japan Earthquake Disaster.

Key Words: Tohoku earthquake, Great East Japan Earthquake Disaster, seismology, geodesy

INTRODUCTION

A super large earthquake occurred on 11 March 2011 (UTC) in the subduction zone along the Japan Trench. This earthquake was officially named "2011 off the Pacific coast of Tohoku Earthquake" by the Japan Meteorological Agency (JMA, 2011a), but we abbreviate it as "2011 Tohoku earthquake" because of its awkward length. Its moment magnitude (M_w) of 9.0 (JMA, 2011b) to 9.1 (Global CMT Project, 2011) is the largest ever recorded in Japan and the fourth in "Largest Earthquakes in the World Since 1900" compiled by the United States Geological Survey (USGS, 2011a).

The 2011 Tohoku earthquake caused a huge disaster, which was officially named "Great East Japan Earthquake Disaster" by the Cabinet of Japan (2011). This disaster resulted in 16,131 fatalities, 3,240 missing, 5,994 injured, and 128,497 house collapses as of 13 January 2012 including the toll from the aftershocks and triggered events (Fire and Disaster Management Agency of Japan, 2012). The number of fatalities is the second for Japanese earthquakes in "Earthquakes with 1,000 or More Deaths since 1900" (USGS, 2011b), preceded by only the 1923 Kanto earthquake. Therefore, the most striking general feature of the 2011 Tohoku earthquake and Great East Japan Earthquake Disaster is of course their hugeness.

The 2011 Tohoku earthquake is a megathrust event in a subduction zone like most others in the list of "Large Earthquakes in the World Since 1900" but the first that was observed by dense networks of geophysical instruments. This is the first specific feature of the earthquake and disaster. Since more than 90% of the fatalities were from drowning (Kyodo News, 2011), and the number of injured people is relatively small, the second specific feature of the earthquake and disaster is severe tsunami damage but moderate ground motion damage. Many large aftershocks and triggered earthquakes also caused ground motion damage. The third specific feature is that the earthquake and disaster had not been foreseen at all. We will explain these specific features in turn as the seismological and geodetic aspects of the 2011 Tohoku earthquake and Great East Japan Earthquake Disaster.

OBSERVED BY DENSE NETWORKS OF GEOPHYSICAL INSTRUMENTS

Abundant data obtained from the dense networks include teleseismic, strong motion, geodetic, and tsunami datasets. For example, the strong motion seismometers of K-NET and KiK-net (National Research Institute for Earth Science and Disaster Prevention (NIED), 2008) observed ground accelerations from the earthquake at stations shown in Fig. 1A. Gauges that observed the tsunami are also shown in Fig. 1A with the associated waveforms, though many of these stations stopped recording early because of power failure or tsunami damage. The tsunami dataset consists of these waveforms and observations at remote stations (Fujii *et al*., 2011). The GEONET (Geospatial Information Authority of Japan (GSI), 2010), which is a nation-wide network of 1,200 GPS-based control stations, observed crustal deformations due to the earthquake as shown by static displacements in Fig. 2.

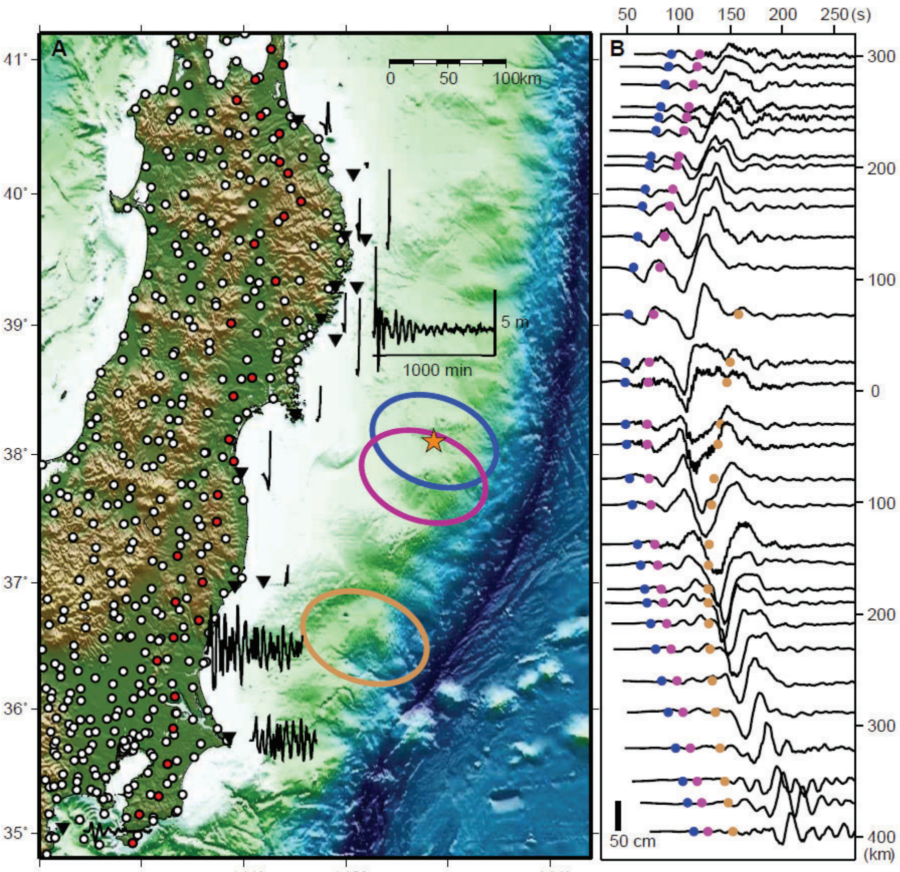

Fig. 1. (A) Strong motion stations operated by NIED (small white and red circles) and local tsunami gauges (black inverted triangles) associated with observed waveforms (black traces). The orange star denotes the epicenter determined by JMA (2011c). (B) Section of ground displacements obtained by double integration of accelerations observed at the red stations. Three pulses can be seen and their arrival times (blue, red, and brown dots) suggest three zones of large slip (blue, red, and brown ellipses in the panel A (Koketsu *et al*., 2011).

The strong motion records at 31 stations selected along the Pacific coast (red circles in Fig. 1A) were doubly integrated into ground displacements using highpass filter with a corner period of 100 s.

They were aligned along the coast to form the record section in Fig. 1B. Three pulses, two of which are distinct but the other is not, can be seen in this record section, and their arrival times indicated by blue, red, and brown dots suggest that they were generated in the zones drawn with the same colors in Fig. 1A. The first two zones are located around the epicenter of the mainshock determined by JMA (2011c), while the third zone is 150 to 180 km south of the epicenter. The static displacements in Fig. 2 point toward these zones, though they cannot distinguish the first two zones because of their limited resolving power.

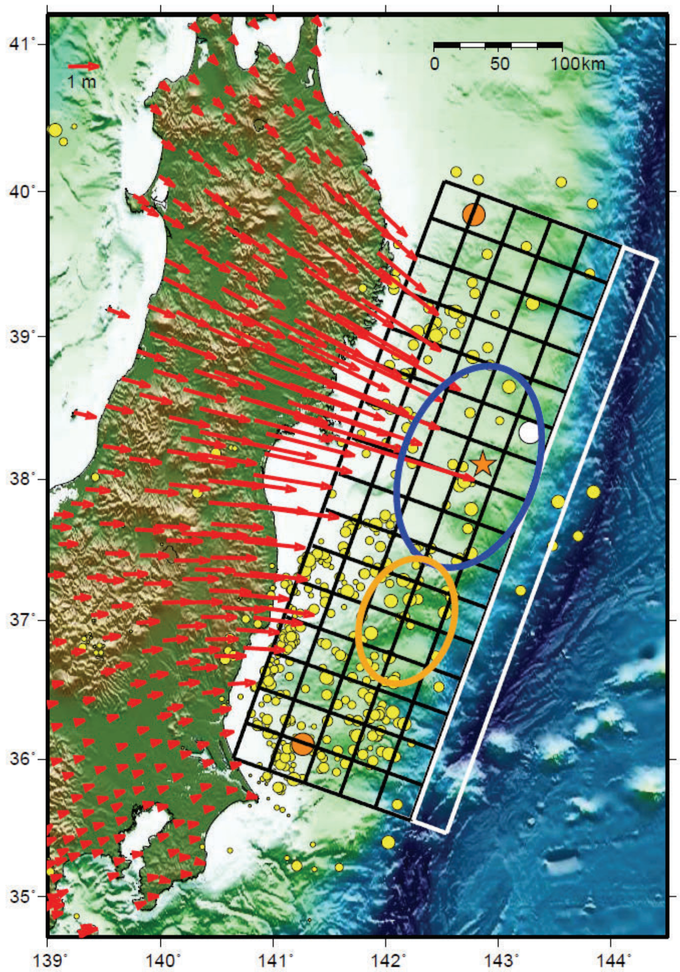

Fig. 2. Horizontal static displacements observed by GEONET (red arrows) suggest two zones of large slip (blue and brown ellipses). The source fault (rectangular grid) is assumed based on the distribution of smaller earthquakes during the initial 24 hours (yellow circles). The orange star, orange and white circles denote the epicenters of the mainshock, aftershocks with magnitudes greater than 7.0, and a foreshock, respectively. The white narrow rectangle is an extension of the source fault for the tsunami inversion (Koketsu *et al*., 2011).

Fig. 2 also shows smaller earthquakes in the 24 hours after the mainshock of the Tohoku earthquake. We considered those in the black rectangular grid to be aftershocks and this rectangle of 480 × 150 km^2 was adopted with a strike of 200° and a dip of 12° to model the source fault of the mainshock. The two large events with JMA magnitudes of 7.7 and 7.4 (JMA, 2011c) were included, but some events adjacent to the western side of the rectangle were excluded, because their depths (5 to 30 km) are much shallower than the depth of the upper boundary of the subducting Pacific plate beneath them (50 to 70 km in the Japan Integrated Velocity Structure Model (JIVSM) (Koketsu *et al*., 2008). On the eastern side, there is a gap between the model rectangle and the axis of the Japan Trench, as shown by a white narrow rectangle. However, we did not extend the source fault model to this area for the inversions of teleseismic, strong motion, and geodetic datasets, because there was almost no seismicity there in the 24 hours after the mainshock. Another reason is that only the 1896 Sanriku earthquake is known to be a large plate-boundary event in this area and it is a typical tsunami earthquake which radiates small seismic energy but large tsunami (Kanamori, 1972; Tanioka and Satake, 1996).

In addition, the strong motion dataset already shows that observed ground motions are smaller than estimates by existing ground motion prediction equations (Si *et al*., 2012; Miyake *et al*., 2012), as shown in Fig. 3. Therefore, a resultant source model can include a reason for the moderate ground motion damage.

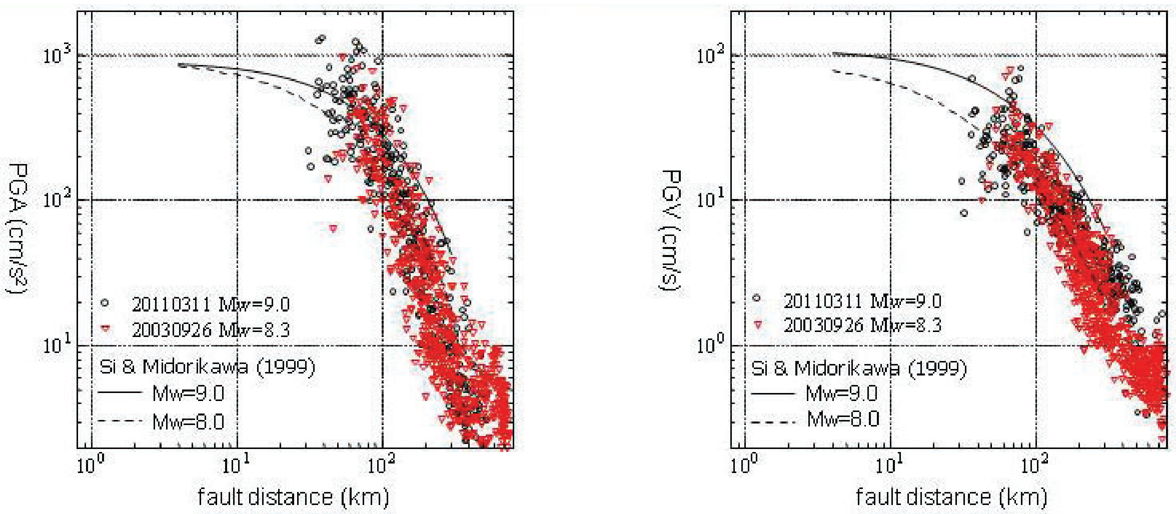

Fig. 3. Comparisons of PGAs (left) and PGVs (right) for the 2011 Tohoku and 2003 Tokachi-oki earthquakes (Si *et al*., 2012).

SEVERE TSUNAMI DAMAGE BUT MODERATE GROUND MOTION DAMAGE

Yokota *et al*. (2011) carried out source inversions of the various datasets mentioned in the previous section. Their results in Fig. 4 indicate that the earthquake consists of three main ruptures. After small bilateral rupture in the initial 40 s (0 – 40 s), the first main rupture propagated to the easternmost shallow area and generated the compact shallow slip (40 – 60 s). Later, the second main rupture began to propagate northwestward and southward and became dominant with the largest final slip of 35 m (60 – 100 s). At this time, the slip propagated to the westernmost area including the Miyagi-oki region. The southward rupture finally reached west off Fukushima Prefecture, approximately 200 km south of the hypocenter during the third main rupture stage (100 – 120 s).

The first and second main ruptures expanded at a slow speed of 1.5 ~ 1.8 km/s. The slow rupture growth of the earthquake source required larger fracture energy, therefore the resultant radiated energy became smaller based on the energy budget (Kanamori and Heaton, 2000). Thus, one feature of the earthquake and disaster, which is moderate ground motion damage, can be explained by the slow rupture speed. The other feature, which is severe tsunami damage, can be explained by large slips close to the Japan Trench (white ellipse in Fig. 4a).

In addition to the super large mainshock, many large aftershocks and triggered earthquakes have occurred causing extra ground motion damage (Fig. 5). The JMA defined the 600 × 350 km^2 aftershock area and is counting the numbers of aftershocks with various JMA magnitudes (*M*). Six *M*7, ninety *M*6, and four hundred eighty four *M*5 aftershocks were reported to occur from 11 March 2011 to 10 January 2012. Among the above *M*7 events in 2011, *M*7.5 on 11 March, *M*7.2 on 7 April, and

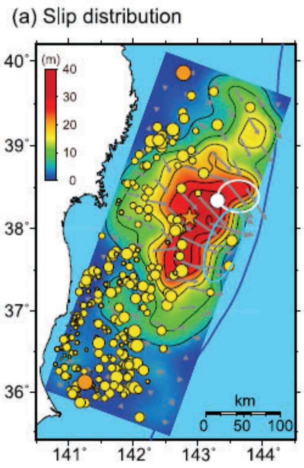

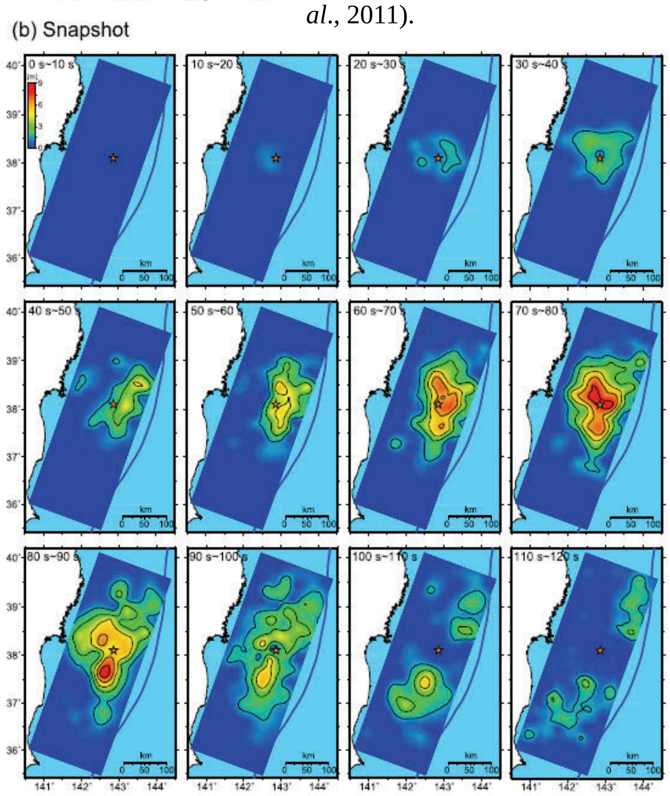

Fig. 4. (a) Slip distributions obtained by a joint inversion. The yellow circles denote aftershocks in the initial 24 hours. The orange star and the orange and white circles denote the epicenter of the mainshock, aftershocks with magnitudes greater than 7.0, and a foreshock, respectively. The white ellipse denotes shallow large slips. (b) The progress of the source rupture is represented by the snapshots of the slip distribution every 10 s after rupture initiation (Yokota *et al.*, 2011).

*M*7.1 on 11 April have focal mechanisms different from that of the mainshock. Thus, in a narrow sense, they are not aftershocks but triggered earthquakes like the events far away from the aftershock area (Fig. 5), though the *M*7.2 and *M*7.1 events close to the Tohoku district caused ground motion damage.

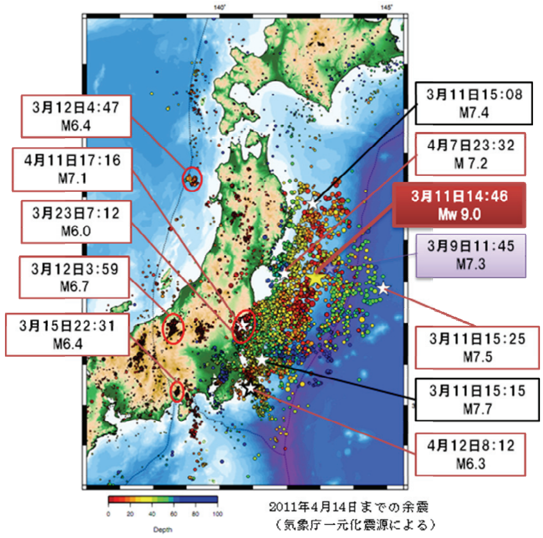

Fig. 5 Earthquakes from 11 March to 14 April 2011 including the mainshock (yellow star), foreshock (purple star), aftershocks (black boxes), and triggered earthquakes (red boxes) (by Drs. Oki and Nishida).

Triggered inland earthquakes such as the *M*6.7 on 12 March and *M*6.4 on 15 March also caused ground motion damage.

THEY HAD NOT BEEN FORESEEN AT ALL

The 2011 Tohoku earthquake is a megathrust event along the Japan Trench, where the Pacific plate is subducting beneath the Tohoku district. The national seismic hazard assessment program, which had been initiated by the Japanese government after the 1995 Kobe earthquake (Headquarters for Earthquake Research Promotion, 1999) based on the characteristic earthquake model (Schwartz and Coppersmith, 1984) and the asperity model (Lay and Kanamori, 1981), was unable to foresee this earthquake (Geller, 2011). For example, the program merely identified a cycle of six *M*7 to *M*8 characteristic earthquakes in the landside of the Miyagi-oki region; further, the program only reported the high probability of another *M*7 earthquake occurrence in the region (Fig. 6).

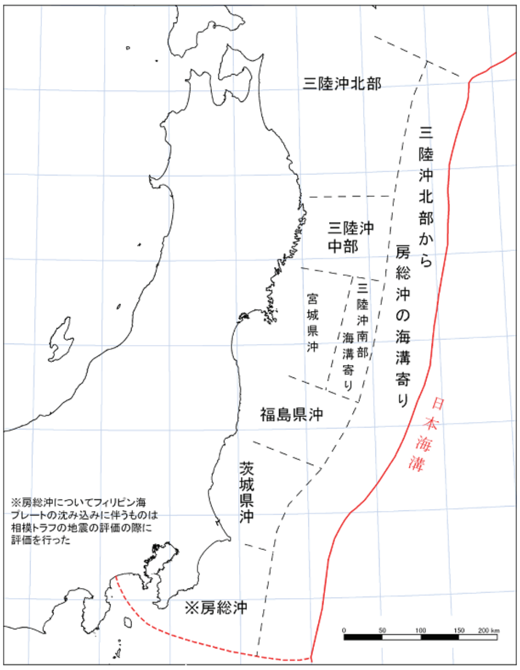

三陸沖から房総沖にかけての地震	三陸沖から房総沖の海溝寄り	津波地震	Mt8.2前後（Mtは津波の高さから求める地震の規模）		20%程度（6%程度）*
		正断層型	8.2前後		4%～7%（1%～2%）*
	三陸沖北部		8.0前後		0.5%～10%
		固有地震以外のプレート間地震	7.1～7.6		90%程度
	宮城県沖		7.5前後	連動8.0前後	99%
	三陸沖南部海溝寄り		7.7前後		80%～90%
	福島県沖		7.4前後（複数の地震が続発する）		7%程度以下
	茨城県沖		6.7～7.2		90%程度以上

Fig. 6. Results of the national seismic hazard assessment program for the Tohoku district (Earthquake Research Committee, 2005).

In addition, the Japanese government installed nation-wide dense arrays of seismometers and GPS receivers (Figs. 1 and 2) after the Kobe earthquake (Headquarters for Earthquake Research Promotion, 1999). In their study, Nishimura *et al*. (2004) estimated the annual rates of back slip (defined as the drag of the overriding plate due to interplate coupling) using GPS data during a calm period before the 2011 Tohoku earthquake. The coseismic slip distribution by Koketsu *et al.* (2011) bears a close resemblance to the distribution of these back slip rates (Fig. 7). According to previous studies, an area with large back slip rates was thought to be related to characteristic earthquakes. However, our result demonstrates that such an area is related to a megathrust earthquake.

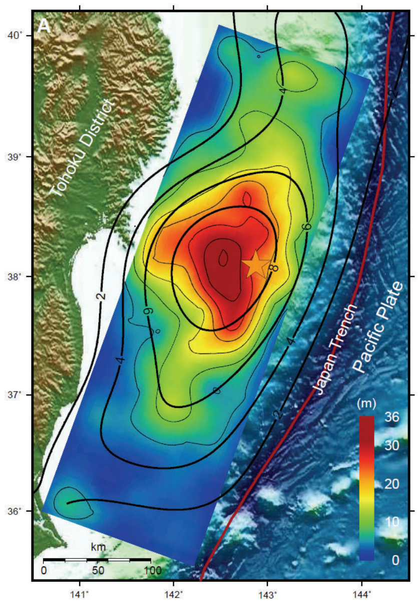

Fig. 7. Comparison of the distributions of coseismic slips during the 2011 Tohoku earthquake and back slip rates by Nishimura *et al*. (2004).

Therefore, we believe that the 2011 Tohoku earthquake could have been foreseen with respect to at least its location and extent if the GPS array data had been monitored considering their relation to a megathrust earthquake. We also believe that this foreseeability can be applied to megathrust earthquakes in other subduction zones where GPS arrays have been installed. Subsequently, it is the most important for seismic hazard assessments in these subduction zones to identify past megathrust earthquakes.

CONCLUSIONS

We have pointed out the one general feature and three specific features of the 2011 Tohoku earthquake and Great East Japan Earthquake Disaster. We have then explained the details of the three specific features as the seismological and geodetic aspects of the 2011 Tohoku earthquake and Great East Japan Earthquake Disaster.

REFERENCES

Cabinet of Japan (2011). Press Conference by Prime Minister Naoto Kan (http://www.kantei.go.jp/foreign/kan/statement/201104/01kaiken_e.html).

Earthquake Research Committee (2005). *National Seismic Hazard Maps for Japan*, (http://www.jishin.go.jp/main/chousa/06mar_yosoku-e/NationalSeismicHazardMaps.pdf).

Fire and Disaster Management Agency of Japan (2012). The 143rd report (13 January 2012) (http://www.fdma.go.jp/bn/2012/detail/691.html).

Fujii, Y., Satake, K., Sakai, S., Shinohara, M. and Kanazawa, T. (2011). Tsunami source of the 2011 off the Pacific coast of Tohoku, Japan earthquake, *Earth Planets Space*, **63**, 815-820.

Geller, R. J. (2011). Shake-up time for Japanese seismology, *Nature*, **472**, 407-409.

Global CMT Project (2011). Global CMT Catalog Search (http://www.globalcmt.org/CMTsearch.html).

GSI (2010). Geodetic survey (http://www.gsi.go.jp/ENGLISH/page_e30030.html).

Headquarters for Earthquake Research Promotion (1999). *The Promotion of Earthquake Research*, (http://www.jishin.go.jp/main/suihon-e/sogo.pdf).

JMA (2011a). On the Sanriku-oki earthquake at 14:46 on 11 March 2011 ~2nd report~ (http://www.jma.go.jp/jma/press/1103/ 11c/201103111620.html).

JMA (2011b). The 2011 off the Pacific coast of Tohoku Earthquake ~28th report~ (http://www.jma.go.jp/jma/press/1103/25b/201103251730.html).

JMA (2011c). Seismological and Volcanological Bulletin of Japan for March 2011 (http://www.hinet.bosai.go.jp/REGS/JMA/list/).

Kanamori, H. (1972). Mechanism of tsunami earthquakes, *Phys. Earth Planet. Interiors*, **6**, 346-359.

Kanamori, H. and Heaton, T. H. (2000). Microscopic and macroscopic physics of earthquakes, in *GeoComplexity and the Physics of Earthquakes*, Geophysical Monograph **120**, 147-163.

Koketsu, K., Miyake, H., Fujiwara, H., Hashimoto, T. (2008). Progress towards a Japan integrated velocity structure model and long-period ground motion hazard map, *Proceedings of the 14th World Conference on Earthquake Engineering*, S10-038.

Koketsu, K., Yokota, Y., Nishimura, N., Yagi, Y., Miyazaki, S., Satake, K., Fujii, Y., Miyake, H., Sakai, S., Yamanaka, Y. and Okada, T. (2011). A unified source model for the 2011 Tohoku earthquake, *Earth Planet. Sci. Lett.*, **310**, 480-487.

Kyodo News (2011). Over 90% of March 11 victims died from drowning (http://www.japantoday.com/category/national/view/over-90-of-march-11-victims-died-from-drowning-npa).

Lay, T. and Kanamori, H. (1981). An asperity model of large earthquake sequences, in *Earthquake*

Prediction —An international review, Maurice Ewing Series 4, 579-592.

Miyake, H., Yokota, Y., Si, H. and Koketsu, K. (2012). Ground motion aspects of the 2011 Tohoku earthquake: Crack-like ruptures with down-dip short-period phases, *Geophys. Res. Lett.*, in revision.

NIED (2008). (K-NET, KiK-net) (http://www.kyoshin.bosai.go.jp/index_en.html).

Nishimura, T., Hirasawa, T., Miyazaki, S., Sagiya, T., Tada, T., Miura, S. and Tanaka, K. (2004). Temporal change of interplate coupling in northeastern Japan during 1995–2002 estimated from continuous GPS observations, *Geophys. J. Int.*, **157**, 901-916.

Schwartz, D. P. and Coppersmith, K. J. (1984). Fault behavior and characteristic earthquakes: Examples from the Wasatch and San Andreas fault zones, *J. Geophys. Res*., **89**, 5681-5698.

Si, H., K. Koketsu and Miyake, H. (2012). Oversaturation of ground motion from megathrust earthquakes, *Bull. Seismol. Soc. Am.*, submitted.

Lorito, S., Romano, F., Atzori, S., Tong, X., Avallone, A., McCloskey, J., Cocco, M., Boschi, E. and Piatanesi, A. (2011). Limited overlap between the seismic gap and coseismic slip of the great 2010 Chile earthquake, *Nature Geoscience*, **4**, 173-177.

Tanioka, Y. and Satake, K. (1996). Fault parameters of the 1896 Sanriku tsunami earthquake estimated from tsunami numerical modeling, *Geophys. Res. Lett.*, **23**, 1549-1552.

USGS (2011a). Largest Earthquakes in the World Since 1900 (http://earthquake.usgs.gov/earthquakes/world/10_largest_world.php).

USGS (2011b). Earthquakes with 1,000 or More Deaths since 1900 (http://earthquake.usgs.gov/earthquakes/world/world_deaths.php).

Yokota, Y., Koketsu, K., Fujii, Y., Satake, K., Sakai, S., Shinohara, M. and Kanazawa, T. (2011). Joint inversion of strong motion, teleseismic, geodetic, and tsunami datasets for the rupture process of the 2011 Tohoku earthquake, *Geophys. Res. Lett.*, **L00G21**, doi:10.1029/2011GL050098.